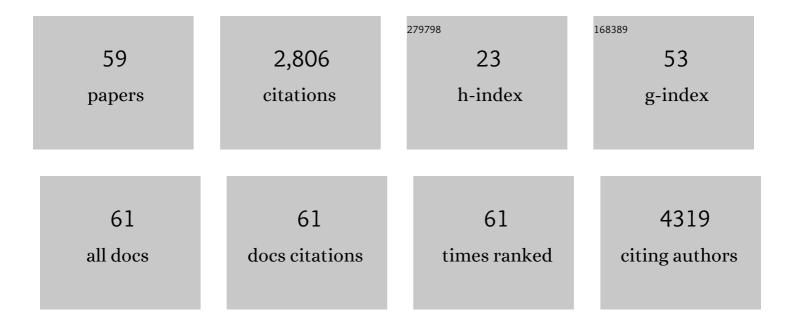
Jaysen Nelayah

List of Publications by Year in descending order

Source: https://exaly.com/author-pdf/1124784/publications.pdf Version: 2024-02-01



#	Article	IF	CITATIONS
1	Effect of size on the surface energy of noble metal nanoparticles from analytical and numerical approaches. Physical Review B, 2022, 105, .	3.2	10
2	Introducing cobalt as a potential plasmonic candidate combining optical and magnetic functionalities within the same nanostructure. Nanoscale, 2021, 13, 2639-2647.	5.6	11
3	Studying the Effects of Temperature on the Nucleation and Growth of Nanoparticles by Liquid-Cell Transmission Electron Microscopy. Journal of Visualized Experiments, 2021, , .	0.3	2
4	Characterization of the boron profile and coordination in altered glass layers by EEL spectroscopy. Micron, 2021, 141, 102983.	2.2	3
5	Corrosion Products Formed on MgZr Alloy Embedded in Geopolymer Used as Conditioning Matrix for Nuclear Waste—A Proposition of Interconnected Processes. Materials, 2021, 14, 2017.	2.9	0
6	Quantitative In Situ Visualization of Thermal Effects on the Formation of Gold Nanocrystals in Solution. Advanced Materials, 2021, 33, e2102514.	21.0	15
7	Revealing Size Dependent Structural Transitions in Supported Gold Nanoparticles in Hydrogen at Atmospheric Pressure. Small, 2021, 17, e2104571.	10.0	13
8	Quantitative Study of Temperature Effects on The Nucleation and Growth of Gold Nanocrystals in Water. Microscopy and Microanalysis, 2021, 27, 29-30.	0.4	0
9	Insights into the Structure-Reactivity of Supported Au Nanocatalyst during Butadiene Selective Hydrogenation by Atomic Scale In Situ Environmental TEM. Microscopy and Microanalysis, 2021, 27, 41-42.	0.4	0
10	Nanoscale temperature measurement during temperature controlled in situ TEM using Al plasmon nanothermometry. Ultramicroscopy, 2020, 209, 112881.	1.9	9
11	On the Influence of Oxygen on the Degradation of Feâ€N Catalysts. Angewandte Chemie, 2020, 132, 3261-3269.	2.0	133
12	On the Influence of Oxygen on the Degradation of Feâ€N Catalysts. Angewandte Chemie - International Edition, 2020, 59, 3235-3243.	13.8	160
13	Selective shortening of gold nanorods: when surface functionalization dictates the reactivity of nanostructures. Nanoscale, 2020, 12, 22658-22667.	5.6	13
14	A deep learning approach for determining the chiral indices of carbon nanotubes from high-resolution transmission electron microscopy images. Carbon, 2020, 169, 465-474.	10.3	27
15	Revealing the Dynamics of Functional Nanomaterials in Their Formation and Application Media with Liquid and Gas-phase TEM. Microscopy and Microanalysis, 2020, 26, 196-198.	0.4	1
16	Quantitative insights into the growth mechanisms of nanopores in hexagonal boron nitride. Physical Review Materials, 2020, 4, .	2.4	8
17	Reshaping Dynamics of Gold Nanoparticles under H ₂ and O ₂ at Atmospheric Pressure. ACS Nano, 2019, 13, 2024-2033.	14.6	32
18	Revealing the Surface Energetics and Reactivity of Bimetallic Copper-Gold Catalyst Nanoparticles by In Situ Environmental TEM. Microscopy and Microanalysis, 2019, 25, 33-34.	0.4	1

JAYSEN NELAYAH

#	Article	IF	CITATIONS
19	Probing the Dynamics and the Atomic Structure of Gold Nanorods in Solution with Liquid-Cell TEM. Microscopy and Microanalysis, 2019, 25, 45-46.	0.4	0
20	Nanostructured Nickel Aluminate as a Key Intermediate for the Production of Highly Dispersed and Stable Nickel Nanoparticles Supported within Mesoporous Alumina for Dry Reforming of Methane. Molecules, 2019, 24, 4107.	3.8	25
21	Structural analysis of single nanoparticles in liquid by low-dose STEM nanodiffraction. Micron, 2019, 116, 30-35.	2.2	7
22	Disentangling the Degradation Pathways of Highly Defective PtNi/C Nanostructures – An Operando Wide and Small Angle X-ray Scattering Study. ACS Catalysis, 2019, 9, 160-167.	11.2	22
23	Thermodynamics of faceted palladium(–gold) nanoparticles supported on rutile titania nanorods studied using transmission electron microscopy. Physical Chemistry Chemical Physics, 2018, 20, 13030-13037.	2.8	3
24	Direct Measurement of the Surface Energy of Bimetallic Nanoparticles: Evidence of Vegard's Rulelike Dependence. Physical Review Letters, 2018, 120, 025901.	7.8	19
25	Monitoring the dynamics of cell-derived extracellular vesicles at the nanoscale by liquid-cell transmission electron microscopy. Nanoscale, 2018, 10, 1234-1244.	5.6	28
26	Driving reversible redox reactions at solid–liquid interfaces with the electron beam of a transmission electron microscope. Journal of Microscopy, 2018, 269, 127-133.	1.8	12
27	Structural Properties of Catalytically Active Bimetallic Gold–Palladium Nanoparticles Synthesized on Rutile Titania Nanorods by Pulsed Laser Deposition. Crystal Growth and Design, 2018, 18, 68-76.	3.0	8
28	Effect of Atomic Vacancies on the Structure and the Electrocatalytic Activity of Ptâ€rich/C Nanoparticles: A Combined Experimental and Density Functional Theory Study. ChemCatChem, 2017, 9, 2324-2338.	3.7	23
29	Exploring the Formation of Symmetric Gold Nanostars by Liquid-Cell Transmission Electron Microscopy. Nano Letters, 2017, 17, 4194-4201.	9.1	56
30	Atomic-Scale Snapshots of the Formation and Growth of Hollow PtNi/C Nanocatalysts. Nano Letters, 2017, 17, 2447-2453.	9.1	40
31	Implementing Structural Disorder as a Promising Direction for Improving the Stability of PtNi/C Nanoparticles. ACS Catalysis, 2017, 7, 3072-3081.	11.2	61
32	Hydrogen absorption in 1Ânm Pd clusters confined in MIL-101(Cr). Journal of Materials Chemistry A, 2017, 5, 23043-23052.	10.3	33
33	(Invited) Porous Hollow PtNi/C Nanoparticles and Their Many Facets. ECS Transactions, 2017, 80, 731-741.	0.5	2
34	Structural Transformations of Au and Au-Cu Nanoparticles during Liquid-Phase Synthesis and Redox Reactions in Gaseous Environment. Microscopy and Microanalysis, 2017, 23, 1860-1861.	0.4	0
35	Structure–Activity Relationships for the Oxygen Reduction Reaction in Porous Hollow PtNi/C Nanoparticles. ChemElectroChem, 2016, 3, 1591-1600.	3.4	16
36	Defects do Catalysis: CO Monolayer Oxidation and Oxygen Reduction Reaction on Hollow PtNi/C Nanoparticles. ACS Catalysis, 2016, 6, 4673-4684.	11.2	107

JAYSEN NELAYAH

#	Article	IF	CITATIONS
37	Ostwald-Driven Phase Separation in Bimetallic Nanoparticle Assemblies. ACS Nano, 2016, 10, 4127-4133.	14.6	19
38	Monitoring Extracellular-Vesicles Dynamics at the Nanoscale by Liquid-Cell TEM. Microscopy and Microanalysis, 2016, 22, 32-33.	0.4	2
39	Au–Rh and Au–Pd nanocatalysts supported on rutile titania nanorods: structure and chemical stability. Physical Chemistry Chemical Physics, 2015, 17, 28112-28120.	2.8	42
40	Tuning the Performance and the Stability of Porous Hollow PtNi/C Nanostructures for the Oxygen Reduction Reaction. ACS Catalysis, 2015, 5, 5333-5341.	11.2	125
41	New insights into the mixing of gold and copper in a nanoparticle from a structural study of Au–Cu nanoalloys synthesized via a wet chemistry method and pulsed laser deposition. Physical Chemistry Chemical Physics, 2015, 17, 28339-28346.	2.8	25
42	Nanoalloying bulk-immiscible iridium and palladium inhibits hydride formation and promotes catalytic performances. Nanoscale, 2014, 6, 9955-9959.	5.6	40
43	Original Anisotropic Growth Mode of Copper Nanorods by Vapor Phase Deposition. Crystal Growth and Design, 2014, 14, 6350-6356.	3.0	13
44	Long-range chemical orders in Au–Pd nanoparticles revealed by aberration-corrected electron microscopy. Nanoscale, 2014, 6, 10423-10430.	5.6	25
45	Selective hydrogenation of butadiene over TiO ₂ supported copper, gold and gold–copper catalysts prepared by deposition–precipitation. Physical Chemistry Chemical Physics, 2014, 16, 26514-26527.	2.8	67
46	Performances of an 80–200 kV microscope employing a cold-FEG and an aberration-corrected objective lens. Microscopy (Oxford, England), 2013, 62, 283-293.	1.5	41
47	Following Ostwald ripening in nanoalloys by high-resolution imaging with single-atom chemical sensitivity. Applied Physics Letters, 2012, 101, 121920.	3.3	22
48	Plasmon Spectroscopy and Imaging of Individual Gold Nanodecahedra: A Combined Optical Microscopy, Cathodoluminescence, and Electron Energy-Loss Spectroscopy Study. Nano Letters, 2012, 12, 4172-4180.	9.1	139
49	Transition from core–shell to Janus chemical configuration for bimetallic nanoparticles. Nanoscale, 2012, 4, 3381.	5.6	163
50	Low-loss EFTEM Imaging of Surface Plasmon Resonances in Ag Nanostructures. Microscopy and Microanalysis, 2010, 16, 1438-1439.	0.4	1
51	EFTEM study of surface plasmon resonances in silver nanoholes. Ultramicroscopy, 2010, 110, 1094-1100.	1.9	16
52	Thickness dependent microstructural changes in La0.5Ca0.5MnO3 thin films deposited on (111) SrTiO3. Thin Solid Films, 2010, 518, 4667-4669.	1.8	2
53	Two-Dimensional Quasistatic Stationary Short Range Surface Plasmons in Flat Nanoprisms. Nano Letters, 2010, 10, 902-907.	9.1	103
54	Mapping of valence energy losses via energy-filtered annular dark-field scanning transmission electron microscopy. Ultramicroscopy, 2009, 109, 1164-1170.	1.9	28

JAYSEN NELAYAH

#	Article	IF	CITATIONS
55	Direct imaging of surface plasmon resonances on single triangular silver nanoprisms at optical wavelength using low-loss EFTEM imaging. Optics Letters, 2009, 34, 1003.	3.3	77
56	Electron energy losses in Ag nanoholes—from localized surface plasmon resonances to rings of fire. Optics Letters, 2009, 34, 2150.	3.3	44
57	Application of Monochromated Electrons in EELS. Microscopy and Microanalysis, 2008, 14, 134-135.	0.4	2
58	Mapping surface plasmons on a single metallic nanoparticle. Nature Physics, 2007, 3, 348-353.	16.7	908
59	Probing surface plasmons on individual nano-objects by near-field electron energy loss spectroscopy. , 2005, , .		2